

# Boundary induced convection in a collection of polar self-propelled particles

Shradha Mishra\*

Department of Physics, Indian Institute of Technology (BHU), Varanasi, India 221005

Sudipta Pattanayak

S N Bose National Centre for Basic Sciences, J D Block, Sector III, Salt Lake City, Kolkata 700098

(Dated: September 4, 2021)

We study a collection of polar self-propelled particles confined to a long two-dimensional channel. We write the coupled hydrodynamic equations of motion for density and polarisation order parameter. At two confined boundaries, density is fixed to the mean and orientation is anti-parallel with fixed magnitude of polarisation. Such boundary conditions make our system similar to a sheared suspension of self-propelled particles, which has many practical applications. Antiparallel alignment at the two confined boundaries and alignment inside the channel create *rolls* of orientation along the long axis of the channel. For zero self-propulsion speed, density and orientation fields are decoupled and density remains homogeneous inside the channel. For finite self-propelled speed, density inhomogeneities develop and these *rolls* move along the long axis of the channel. Density inhomogeneity increases sharply with increasing the self propulsion speed and then reaches a maximum and again decreases for very large speeds. Formation of *rolls* is very similar to the classic problem of Rayleigh-Benard convection in fluid dynamics.

## I. INTRODUCTION

Collective behaviour of active particles are extensively studied in [1–4]. Large collections of living organisms are known to exhibit highly coherent collective motion [5–9] This behavior, often referred to as “flocking” spans an enormous range of length scales and is seen in diverse systems [10–20]. These systems are regoursly studied in *bulk* either (i) using hydrodynamic equations of motion for slow variables (ii) or microscopic rule based models *viz.*: Vicsek’s model [5]. *But* most biological systems are confined to thin geometry [21]. Confinement and boundary plays an important role in variety of problems in biology [21], sheared systems [22] and other places like in fluid dynamics. One classic example include Rayleigh-Benard (RB) convection in fluid [23]. In these confined systems, the effect of boundaries are very important.

Boundary can play very important role in a collection of self-propelled particles. It can induce many interesting phenomena like, in many cases, boundary can induce spontaneous flow inside the channel [24]. We write the phenomenological equations of motion for local density and polarisation order parameter for the collection of polar self-propelled particles Eqs. 1 and 2. Self-propelled speed (SPS) of the particle introduces a non-equilibrium coupling between density and polarisation. For zero SPS both density and polarisation are decoupled. We solve these equations in the confined geometry shown in Fig. 2. At the two boundaries of the channel orientation of rods are antiparallel, which produces a gradient along the confinement direction. Diffusion tries to make them parallel. Hence the competition between above two

create *rolls* of orientation along the long-axis of the channel. For zero SPS these rolls are static and density inside the channel is homogeneous. For non-zero SPS both density and polarisation are coupled and such coupling produces moving rolls.

In Fig. 1, we show the (left) vector plot of orientation and (right) density of particles inside the channel for SPS  $v_0 = 1.5$  or activity  $R_A = 0.67'$  at different times. We find inhomogeneous moving pattern of orientation and density along the long axis of the channel Fig. 1(top to bottom). Arrow indicate the direction of motion. In rest of the article, section II discusses the model in detail. Here we also write the hydrodynamic equations of motion for density and polarisation. Section III discusses the numerical details for solving these equations. We discuss our results in section IV and finally conclude with discussion and future aspect of this study in section V.

## II. MODEL

We consider a collection of self-propelled particles of length  $l$  confined to a two-dimensional channel whose thickness  $d$  is very small compare to its long axis  $L$ . We fix the length of the channel  $L$  and vary the width of the channel  $d \ll L$ . Orientation at the lower boundary is parallel to horizontal axis and at the upper boundary it is antiparallel and magnitude of polarisation fixed at two boundaries. We also maintain mean density at two confined boundaries to avoid accumulation of particles at boundaries. Periodic boundary condition is used for both density and polarisation along the long axis of the channel. Geometry of confined channel and orientation of particles at the two boundaries is shown in Fig. 2.

\* smishra.phy@itbhu.ac.in

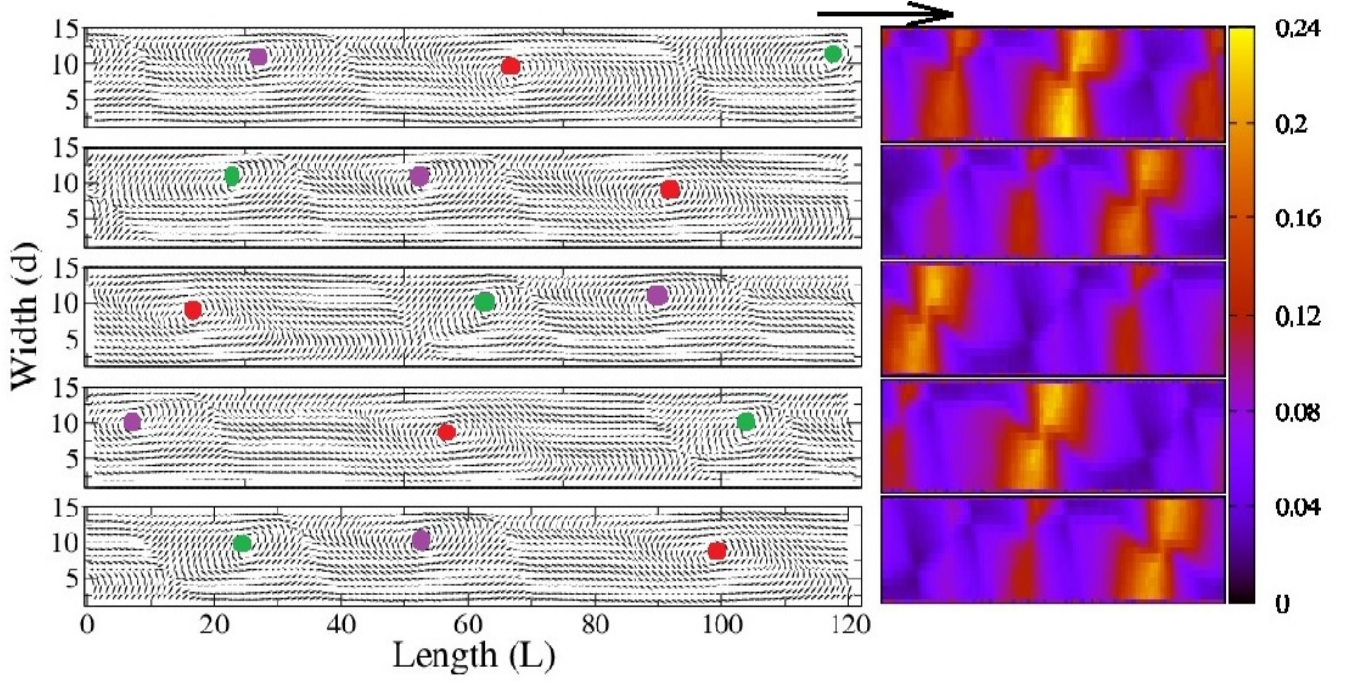


FIG. 1. (Color online) (left) Vector plot of local polarisation and (right) density inside the channel for activity  $R_A = 0.67$ . Different plots are snapshot of polarisation and density at different times. (left) local polarisation shows vortex type periodic pattern (*rolls*) along the long axis of the channel. Different color dots on periodic *rolls* represent distinct vortex. Density also shows periodic pattern. Bright regions are high density and dark regions are low density. Top to bottom figures are from small to large time. With time periodic *rolls* for both density and local polarisation moves from one end to other end of the channel. Arrow on the top of the figure represent direction of motion of periodic pattern. This direction is spontaneously chosen from two equally possible direction in the system.

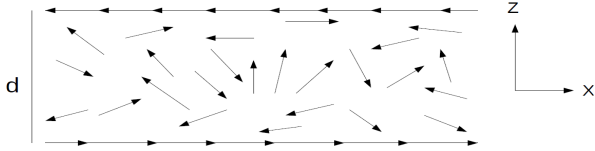


FIG. 2. Geometry of confined channel and orientation of particle at the two confined boundaries.  $x$ -direction is chosen along the long axis of the channel and  $z$ -direction is the confinement direction. Periodic boundary condition is used along the long axis of the channel. Orientation is parallel to  $+x$ -direction at bottom boundary ( $z=1$ ) and parallel to  $-x$ -direction at top boundary ( $z=d$ ). Magnitude of polarisation  $|P| = 1$  is fixed at two boundaries and density is maintained to value  $\rho_0 = 0.1$ .

### A. Hydrodynamic equations of motion

Dynamics of the system is described by the equations of motion for hydrodynamic variables for the collection of polar self-propelled particles. We write the phenomenological coupled hydrodynamic equations of motion for density  $\rho$ , because total number of particles are conserved and polarisation  $P$ , which is an orientation order param-

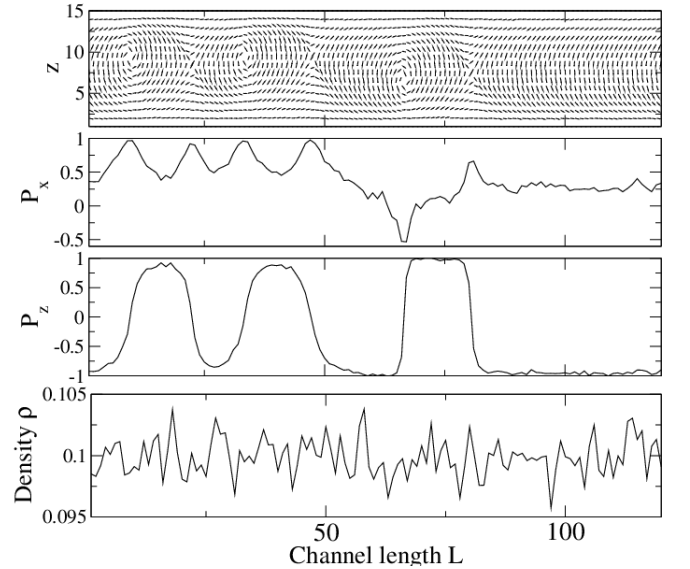


FIG. 3. For zero activity  $R_A = 0$  or SPS  $v_0 = 0.0$ : (a) vector plot of orientation field, which shown periodic vortex type pattern *rolls*. (b)  $x$ -component of polarisation  $P_x$  (c)  $z$ -component of polarisation  $P_z$  and (d) density  $\rho(x)$ : along the long axis of the channel, averaged over the  $z$ -direction.

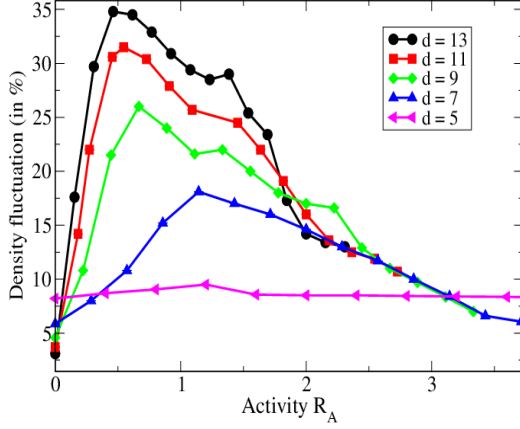


FIG. 4. (color online) Plot of percentage density fluctuation  $\% \Delta N$  vs. activity  $R_A$  for different width  $d$  of the channel.  $\Delta N$  shows non monotonic behaviour as we increase activity  $R_A$ . Density inhomogeneity increases as we increase width of the channel.

eter, is a broken symmetry variable in the ordered state. We write the minimum order terms allowed by symmetry. Two equations are

$$\frac{\partial \rho}{\partial t} = -v_0 \nabla \cdot (\rho \mathbf{P}) + D_\rho \nabla^2 \rho \quad (1)$$

and

$$\frac{\partial \mathbf{P}}{\partial t} = -D_R(-\alpha_0 + \alpha_1 |P|^2) \mathbf{P} - \frac{v_0}{2\rho_0} \nabla \rho + D_P \nabla^2 \mathbf{P} \quad (2)$$

Density equation 1 is a continuity equation because total number of particles are conserved. Right hand side of Eq. 1 can be written as a divergence of a current  $\mathbf{J}$  which has two parts,  $\mathbf{J} = \mathbf{J}_a + \mathbf{J}_p$ , where  $\mathbf{J}_p \propto \nabla \rho$  is proportional to gradient in density we call it “passive current” and  $\mathbf{J}_a \propto v_0 \rho \mathbf{P}$  is proportional to polarisation vector  $\mathbf{P}$  and self-propelled speed  $v_0$  and we call it as “active current”. For zero SPS  $v_0 = 0$  or polarisation  $\mathbf{P} = 0$  active current is zero.

The order parameter equation 2 contains (i) mean field order disorder terms  $\alpha_0$  and  $\alpha_1$ , (ii) pressure term present because of density fluctuation and (iii) diffusion in polarisation  $D_P$ .  $\alpha_0$  and  $\alpha_1$  are positive and determine the mean field value of polarisation  $\mathbf{P}$  in the bulk  $|P| = \sqrt{\frac{\alpha_0}{\alpha_1}}$ . We choose  $\alpha_0 = \alpha_1 = 1.0$ , such choice of  $\alpha_0$  and  $\alpha_1$  prefers homogeneous polarised steady state  $|\mathbf{P}| = 1.0$  in the bulk.  $\nabla \rho$  is the pressure term and proportional to the self-propelled speed  $v_0$  of the particle.  $D_P$  term is written in the limit of equal elastic constant approximation for splay and bend deformations in two dimensions and  $D_R$  is the rotational diffusion.

We rescale all lengths by particle length  $l$  (which we

choose 1) and time by rotational diffusion time  $D_R^{-1}$ .

$$\begin{aligned} r' &= r/l; \\ t' &= t D_R. \end{aligned} \quad (3)$$

and write the dimensionless equations of motion for density

$$\frac{\partial \rho}{\partial t} = -R_A \nabla \cdot (\rho \mathbf{P}) + \bar{D}_\rho \nabla^2 \rho \quad (4)$$

and polarisation order parameter

$$\frac{\partial \mathbf{P}}{\partial t} = (\alpha_0 - \alpha_1 |P|^2) \mathbf{P} - \frac{R_A}{2\rho_0} \nabla \rho + \bar{D}_P \nabla^2 \mathbf{P}. \quad (5)$$

where

$$R_A = \frac{v_0}{l D_R} \quad (6)$$

is the dimensionless activity. It is a ratio between the self-propelled speed  $v_0$  and the rotational diffusion  $D_R$ . Hence we can increase activity either by increasing speed  $v_0$  or having small  $D_R$ . We can also define dimensionless diffusions.

$$\bar{D}_{\rho, P} = \frac{D_{\rho, P}}{l^2 D_R}. \quad (7)$$

which is again ratio between bulk diffusion and rotational diffusion.

### III. NUMERICAL STUDY

We numerically solve the coupled hydrodynamic equations of motion for density and polarisation order parameter. We go beyond mean field and add Gaussian random white noise to the density

$$\frac{\partial \rho}{\partial t} = -R_A \nabla \cdot (\rho \mathbf{P}) + \bar{D}_\rho \nabla^2 \rho + \nabla \cdot \mathbf{f}_\rho(\mathbf{r}, t) \quad (8)$$

and the order parameter

$$\frac{\partial \mathbf{P}}{\partial t} = -(-\alpha_0 + \alpha_1 |P|^2) \mathbf{P} - \frac{R_A}{2\rho_0} \nabla \rho + D_P \nabla^2 \mathbf{P} + \mathbf{f}_P(\mathbf{r}, t) \quad (9)$$

random forces are chosen to have zero mean and correlations

$$\langle f_\rho^i(\mathbf{r}, t) f_\rho^j(\mathbf{r}', t') \rangle = 2\Delta_\rho \delta_{ij} \delta(\mathbf{r} - \mathbf{r}') \delta(t - t') \quad (10)$$

and

$$\langle f_P^i(\mathbf{r}, t) f_P^j(\mathbf{r}', t') \rangle = 2\Delta_P \delta_{ij} \delta(\mathbf{r} - \mathbf{r}') \delta(t - t') \quad (11)$$

where  $\Delta_\rho$  and  $\Delta_P$  are dimensionless noise strengths. Numerical study is done for fix noise strength  $\Delta_\rho = \Delta_P = 0.05$ . We fix  $D_R = 0.1$ , mean density  $\rho_0 = 0.1$ , diffusivities  $D_\rho = D_P = 1.0$ . Hence activity  $R_A$  is varied by changing the SPS  $v_0$ . Typical diffusive length scale in

the system  $\delta = \sqrt{\frac{D_P}{D_R}}$  and for the above specific choice of parameters  $\delta = \sqrt{10} \simeq 3.5$ . Hence, we choose the lower limit on  $d > \delta$  such that  $d$  is not much bigger than  $\delta$  and upper limit such that effect of confinement is important. Hence  $d$  is varied from 5 to 15. We fixed the length of the channel and SPS is changed from zero to large values.

We solve these PDE's 8 and 9 using Euler method for numerical differentiation on a grid  $\Delta x = 1.0$  and  $\Delta t = 0.1$  (we have checked that numerical scheme is convergent and stable for the above choice). Inside the channel we start from initially random order parameter and homogeneous density  $\rho = \rho_0 = 0.1 \pm 0.01$ . At the two boundaries the magnitude of polarisation is fixed to  $P_0 = 1.0$  and antiparallel orientation such that  $P_x(z = 1) = 1.0$ ,  $P_z(z = 1) = 0.0$  and  $P_x(z = d) = -1.0$ ,  $P_z(z = d) = 0.0$  and density is maintained to mean density  $\rho(z = 1) = \rho(z = d) = \rho_0$ . Periodic boundary condition is used along the long axis of the channel.

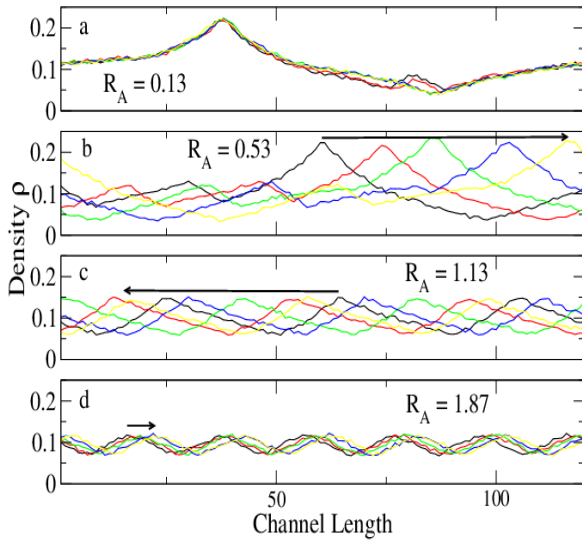


FIG. 5. (color online) Plot of one dimensional density along the long axis of the channel for different self-propelled speeds (a) For small  $R_A = 0.13$ , density shows inhomogeneous structure but with time this inhomogeneous structure does not move much from its position. (b)-(c) For  $R_A = 0.53$  and  $1.13$ , pattern of high and low density move along the long axis of the channel. Patterns move with different speeds at different self-propelled speeds. (d) Again for large  $R_A = 1.87$ , pattern does not move much with time. Density inhomogeneity is small compared to that at intermediate  $R_A$ . Length of the arrow denotes the shift in the density pattern with time

## IV. RESULTS

We divide our results in two parts. First we discuss what happen when activity is turned off, and then we discuss the effect of activity.

### A. Zero activity $R_A = 0$ or SPS $v_0 = 0.0$

For zero activity  $R_A = 0.0$  density and order parameter are decoupled Eqs. 8 and 9. Steady state solution for density is homogeneous density  $\rho = \rho_0$ . Orientation order parameter shows formation of *rolls* along the long axis of the channel. These rolls are formed because of competition between antiparallel boundary condition which produces a gradient in orientation and diffusion term which tries to make them uniform. Mechanism is similar to *Rayleigh-Benard convection* in fluid dynamics, where competition between temperature gradient and gravity produces convective rolls. In Fig. 3 (a) we plot the vector plot of orientation field for zero self-propelled speed  $v_0 = 0.0$ . We find formation of periodic pattern or *rolls* along the long axis of the channel. In Fig. 3(b) and (c) we also plot the  $x$  and  $z$  component of orientation field along the long axis of the channel which confirms the above periodic structure. In Fig. 3 (d) we plot the density along the long axis of the channel, which remains homogeneous inside the channel.

### B. Non-zero activity or SPS $v_0 \neq 0.0$

When we switch on the activity parameter  $R_A$ , hydrodynamic equations of motion for density and polarisation order parameter Eqs. 8 and 9 are coupled. Non-zero activity introduces an active current  $\mathbf{J}_a \propto v_0 \mathbf{P} \rho$  which is proportional to the SPS  $v_0$  and local polarisation  $\mathbf{P}$  (discussed in detail in section II). This active current produces density inhomogeneity and hence enhanced pressure in local polarisation, which is again proportional to SPS  $v_0$  or activity parameter  $R_A$  as shown in Eq. 8 and 9.

#### 1. Density fluctuation

We first calculate the density inhomogeneity for different width of the channel. Density inhomogeneity increases as we increase the width of the channel. In figure 4 we plot the percentage density fluctuation  $\% \Delta \rho$  along the long axis of the channel averaged over transverse direction for five different widths  $d = 5, 7, 9, 11, 13$  as a function of activity parameter  $R_A$ . For very small width  $d = 5$ , density fluctuation is small (*strong confinement*). For width of the channel  $d \geq 7$ , density fluctuation shows non-monotonic behaviour as a function of activity  $R_A$ . As we change  $R_A$  from zero, first increases very sharply with a peak at some finite



$R_A$  and then decreases slowly for larger activity. Peak position shift towards smaller activity as we increase width of the channel. It changes from  $R_A = 1.13$  to  $0.4$  as we change the width from  $d = 7$  to  $d = 13$ . Hence confinement suppresses the large density fluctuation present in general in self-propelled particles in bulk. Suppression of density fluctuation because of confinement is also found previously in the study of sheared suspension of Self-propelled particles [22].

Non-monotonic nature of curve gives a finite range of activity, where fluctuations are large. For very small activity coupling of density to background periodic *rolls* is small and hence small density fluctuation. As we increase activity, active contribution to density current increases: which is proportional to the local order parameter  $\mathbf{P}$  and hence background periodic *rolls* of polarisation order parameter. Activity plays two role here, (i) it produces an active density current proportional to local polarisation. Since such active current creates density inhomogeneity hence (ii) it creates pressure in local polarisation. Hence for very large activity density current will be large but at the same time pressure will also increase and it will destroy the background periodic *rolls*. Hence small active current (because  $\mathbf{J}_a \propto \mathbf{P}$ ), hence small density inhomogeneity.

## 2. Travelling rolls

Even for zero activity as discussed in section IV A, antiparallel boundary conditions at the two confined boundaries creates *rolls* of orientation field. For the range of activity when density fluctuation is large, these *rolls* move from one end to another end of the channel. We call them as *travelling rolls*: where density and orientation both shows periodic pattern (please see fig. 1 for one such activity  $R_A = 0.67$ ). In Fig. 5 we plot density for width of the channel  $d = 13$ , along the long axis of the channel averaged over transverse direction. We calculate density for four different times (with equal time difference) and for four different activity strength  $R_A = 0.13, 0.53, 1.13$  and  $1.87$ . For all activities density shows inhomogeneous periodic pattern. Density inhomogeneity shows variation for different activity. For very small activity  $R_A = 0.13$ , density shows small inhomogeneity and remains static with time. For activity  $R_A = 0.53$ , density is periodic as well as inhomogeneous. These periodic pattern move with time. In Fig. 5(b) we draw a horizontal arrow to denote the motion of periodic pattern with time. Larger the arrow faster the pattern move. Direction of arrow shows the direction of motion of periodic pattern. This direction is spontaneously chosen from two equal possible directions in the system. For activity  $R_A = 1.13$  we get the similar result as for  $R_A = 0.53$  but density inhomogeneity is weaker. For activity  $R_A = 1.87$ , density is periodic but inhomogeneity is even more weak and

very small shift in peak position as a function of time (as shown by small horizontal arrow in Fig. 5(d)). Hence travelling periodic pattern and density inhomogeneity are coupled and larger density inhomogeneity creates faster moving rolls from one end to other end of the channel. For very large activity, density coupling is strong enough such that it destroys the background periodic pattern of orientation and hence no travelling rolls.

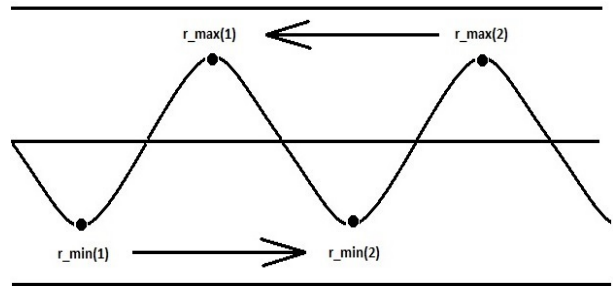


FIG. 6. Cartoon of periodic pattern of density for finite self-propelled speed  $v_0$  or activity  $R_A$ .  $r_{max}[i]$  shows the position of  $i^{th}$  maxima and  $r_{min}[i]$  the position of the  $i^{th}$  minima of density. The two arrows denote the direction of alignment at the two boundaries. We record the position of maxima and minima at different times.

## 3. Mean square displacement

We further characterise properties of *travelling rolls* assuming periodic density pattern as shown in Fig. 5. Cartoon picture of maxima and minima of periodic density profile for one such realization is shown in Fig. 6. We track the position of maxima and minima of periodic density pattern. Position of each maxima and minima we model as position of independent particles moving in one dimension. Hence each maxima and minima represent one particle and we save the position of maxima and minima or particles position with time. We calculate the square displacement of such positions and take average over all maximas and minimas and many initial realisations. Hence mean square displacement is defined as

$$\Delta(t) = \frac{1}{N_e} \sum_{n_e=1}^{N_e} \frac{1}{2} \frac{1}{N_i} \sum_{i=1}^{N_i} [ |r_{max}^{n_e}(i, t_0) - r_{max}^{n_e}(i, t + t_0)|^2 + |r_{min}^{n_e}(i, t_0) - r_{min}^{n_e}(i, t + t_0)|^2 ] \quad (12)$$

where  $r_{max/min}^{n_e}(i, t)$  is the position of maxima/minima of the  $i^{th}$  periodic profile at time  $t$  for  $n_e^{th}$  realisation (as shown in Fig. 6). Averaging is done over all periodic positions  $i = 1, N_i$  and number of realisations  $n_e = 1, N_e$ . For our calculation we used total number of realisation  $N_e = 20$ .

When travelling rolls form as discussed in previous section IV B 2, then  $\Delta(t)$  is proportional to  $t^2$ . In Fig. 7(a) we plot MSD,  $\Delta(t)$  for different activity  $R_A$  for channel of width  $d = 13$ . For zero activity density is homogeneous and no periodic pattern and  $\Delta(t) \simeq t$  (*diffusive*). As we increase activity  $R_A = 0.13$ , MSD  $\Delta(t)$  is *subdiffusion* where  $\Delta(t) \simeq t^\alpha$  and  $\alpha < 1$ . Subdiffusive behaviour shows the arrest of density in the center of the periodic *rolls*, which acts like a disorder site (with small polarisation). Similar arrest of density in the presence of quenched disorder field is found in recent study of [25]. But in our model disorder site or center of the *roll* moves for sufficient large activity. For activity  $R_A \geq 0.67$ , MSD shows two regimes with initial Subdiffusive with  $\alpha < 1$  to later *travelling* motion with  $\alpha \simeq 2$ . Hence for  $R_A \geq 0.67$ , density remains arrested for some time and then travelling rolls sets in. As we further increase activity  $R_A = 0.67$  and  $1.33$  we find initial Subdiffusive with  $\alpha < 1$  and the later travelling motion with  $\alpha = 2$ . Time spent in arrested state decreases as we increase activity. For large activity  $R_A \geq 1.67$ ,  $\Delta(t) \simeq t^\alpha$  for very small time and then switches to transient faster dynamics and then saturates to diffusive  $\Delta(t) \simeq t$  for large time. In Fig. 7(b) we also plot the diffusivity defined as

$$D(t) = \frac{1}{2t} \Delta(t) \quad (13)$$

$D(t)$  remain flat for zero activity, hence *diffusion*. For small activity  $R_A = 0.13$  it decrease with time and shows arrested subdiffusion. For intermediate activities  $R_A = 0.67$  to  $1.33$ ,  $D(t)$  shows initial subdiffusion and later travelling motion with  $D(t) \simeq t$ . For very large activity  $R_A \geq 1.67$  initial  $D(t)$  decreases with time then faster growth to diffusive regime with constant  $D(t)$  for very long time.

We further explain the dynamics of particle inside the channel as we vary the activity  $R_A$ . For zero activity density and orientation are decoupled hence we expect normal diffusive motion for the particle. As we have discussed before antiparallel boundary condition at the two confined boundaries creates periodic *rolls* along the long axis of the channel. As we switch on activity density is coupled to periodic orientation field. For very small activity particles are trapped in periodic orientation. center of periodic pattern acts as quenched disorder site. For intermediate activity coupling is strong and large density inhomogeneity as shown in Fig. 4. Hence for initial transient time particles are trapped to periodic pattern of orientation and later active current sets the travelling *rolls*. Such initial subdiffusion to propagating motion is very common for particle moving in periodic structure. When particle move in a periodic background it spent some of its time in trapped phase and then start propagation. Similar subdiffusion to propagation is found for the particle moving in periodic media [26]. For very large activity coupling is very strong and it destroys the background periodic pattern of orientation and hence diffusive behaviour at late time.

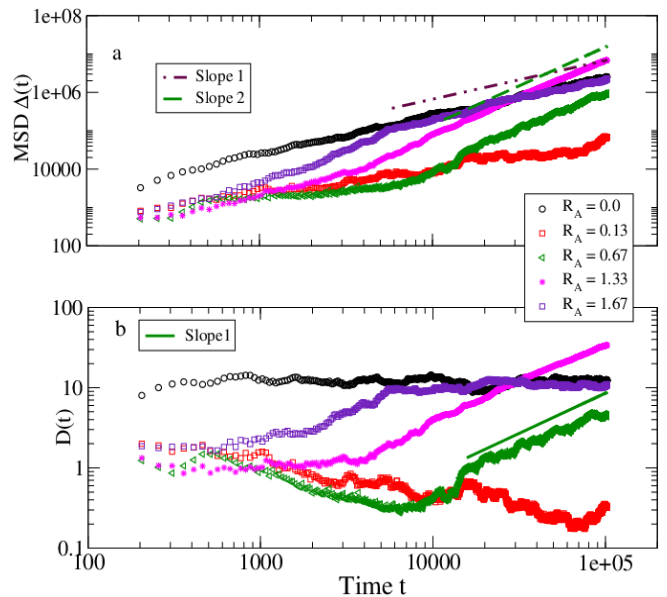


FIG. 7. (color online) plot of (a) mean square displacement (MSD)  $\Delta(t)$  and (b) corresponding diffusion coefficient  $D(t) = \Delta(t)/(2t)$  vs. time  $t$ , of position of high and low density peak position average over many realisation. Different curves are for different activity ranging from  $R_A = 0.0$ , large values  $R_A = 1.67$ . For small  $R_A \leq 0.13$ ,  $\Delta(t) \simeq t$  (a) and density shows diffusive behaviour hence  $D(t)$  approaches constant value (b) at large time. For intermediate  $0.67 \leq R_A < 1.33$ ,  $\Delta(t) \simeq t^2$  and travelling periodic pattern (a) and hence  $D(t) \simeq t$  (b), and for large  $R_A \geq 1.67$ , again diffusive and hence  $\Delta(t) \simeq t$  (a) and  $D(t)$  approaches constant value (b). Two Straight lines in (a) are line of slope 1 and 2. and in (b) straight line is of slope 1.

## V. DISCUSSION

In our present work we write the phenomenological hydrodynamics equations of motion for density and local polarisation order parameter Eq. 8 and 9 for the collection of self-propelled particles. We solve these equation in the confined channel of width  $d \ll L$  very small compare to the long axis of the channel. We impose an antiparallel boundary conditions at the two confinement boundaries and maintain the density at its mean value and the magnitude of polarisation constant. Such a geometry is important because it mimics the shear. First we solved equations(1,2), for zero activity. Antiparallel boundary conditions impose a gradient of orientation along the confinement direction and diffusion tries to make them parallel. Hence there is a competition between these two terms and we find periodic patterns of the orientation field along the long axis of the channel Fig. 3(a). And, since for zero activity density is not coupled to the orientation field, it remains uniform. Non-zero activity, turn on a contribution of active current, which is proportional to the local polarisation

inside the channel. Such active currents make the inhomogeneous density inside the channel. Density inhomogeneity increases as we increase the width of the channel. For fixed channel width, as we increase activity initially density inhomogeneity increases with activity  $R_A$  Fig. 4 and then decrease for large activity  $R_A$ . For fixed channel width, for the range of activity when density inhomogeneity is large, density periodic pattern sets in and start moving from one end to other end of the channel. Real space image of moving periodic orientation *rolls* and density profile for fixed channel width and activity is shown in Fig. 1 for different times. Travelling periodic rolls we observe here is very similar to Rayleigh-Benard convection in fluids. Orientation plays the role of temperature gradient and diffusion is like gravity which acts opposite to gradient. A competition between these two produces periodic rolls and in the

presence of activity these rolls move from one end to other end of the channel.

It would be interesting to study other kinds of boundary condition on the flow properties of active particles inside the channel. For example recent study of [27], where boundary induces accumulation of particles. This phenomena where boundary induces spontaneous flow in confined channel can give some insight of transport of active fluid in biology [28].

## ACKNOWLEDGMENTS

S. Mishra would like to thank DST India for financial support. S. Mishra gratefully acknowledge helpful conversation with Abhik Basu and Argha Banerjee.

- 
- [1] M. Cristina Marchetti *et al.*, Rev. Mod. Phys., **85**, 1143, (2013).
  - [2] Ramaswamy, S., 2010, Annu. Rev. Condens. Matter Phys. 1, 323
  - [3] T Vicsek, A Zafeiris, Physics Reports 517 (3), 71-140 (2012).
  - [4] Toner, J., Y. Tu, and S. Ramaswamy, 2005, Ann. Phys. (Amsterdam) 318, 170
  - [5] T. Vicsek *et al.*, Phys. Rev. Lett. **75**, 1226 (1995).
  - [6] A.Czirok, H. E. Stanley, and T. Vicsek, J. Phys. A **30**, 1375 (1997).
  - [7] J. Toner and Y. Tu, Phys. Rev. Lett. **75**, 4326 (1995); Phys. Rev. E **58**, 4828 (1998),
  - [8] I. Derenyi, P. Tegzes and T. Vicsek "Collective transport in locally asymmetric periodic structures", Traffic and Granular Flow '97, editors M. Schreckenberg and D. E. Wolf (Springer).
  - [9] Shradha Mishra, Aparna Baskaran, and M. Cristina Marchetti Phys. Rev. E **81**, 061916, (2010).
  - [10] *Three dimensional animal groups*, edited by J. K. Parrish and W. M. Hamner (Cambridge University Press, Cambridge, 1997).
  - [11] D. Helbing, I. Farkas, and T. Vicsek, Nature (London) **407**, 487 (2000); Phys. Rev. Lett. **84**, 1240 (2000).
  - [12] T. Feder, Phys. Today 60(10), 28 (2007); C. Feare, The Starlings (Oxford University Press, Oxford, 1984).
  - [13] E. Kuusela, J. M. Lahtinen, and T. Ala-Nissila, Phys. Rev. Lett. 90, 094502 (2003).
  - [14] S. Hubbard, P. Babak, S. Sigurdsson, and K. Magnusson, Ecol. Modell. 174, 359 (2004).
  - [15] E. Rauch, M. Millonas, and D. Chialvo, Phys. Lett. A 207, 185 (1995).
  - [16] E. Ben-Jacob, I. Cohen, O. Shochet, A. Tenenbaum, A. Czirak, and T. Vicsek, Phys. Rev. Lett. 75, 2899 (1995).
  - [17] Y. Harada, A. Nogushi, A. Kishino, and T. Yanagida, Nature (London) **326**, 805 (1987); M. Badoual, F. Jlicher, and J. Prost, Proc. Natl. Acad. Sci. U.S.A. **99**, 6696 (2002).
  - [18] F. J. Ndlec, T. Surrey, A. C. Maggs, and S. Leibler, Nature (London) 389, 305 (1997).
  - [19] Schaller V, Weber C A, Semmerich C, Frey E and Bausch A 2010 Nature 467 73; Schaller V, Weber C, Frey E and Bausch A R 2011 Soft Matter 7 3213; Schaller V, Weber C A, Hammerich B, Frey E and Bausch A R 2011 Proc. Natl Acad. Sci. USA 108 19183.
  - [20] V. Narayan *et al.*, J. Stat. Mech. P01005 (2006); V. Narayan, S. Ramaswamy, and N. Menon, Science **317**, 105 (2007).
  - [21] B. Alberts. Molecular biology of the cell, 4th ed., Garland Science, New York, 2002; R. J. Hawkins *et al.*, Phys. Rev. Lett., 102 (2009), No. 5, 058103;
  - [22] G. P. Saracco, G. Gonnella, D. Marenduzzo, E. Orlandini, Phys. Rev. E 84, 031930 (2011); Eur. J. Phys. 10, 1109 (2012).
  - [23] Bodenschatz, E., Pesch, W. and Ahlers, G., . Annu. Rev. Fluid Mech. **32**, 709, (2000); Busse, F. H. and Clever, R. M., J. Fluid Mech. **91**, 319, (1979).
  - [24] A. Zumdieck *et al.*, Faraday Discussion, **139**, 369, (2008); R.Voituriez, J.F. Joanny and J. Prost, **70**, No. 3, 404, (2005).
  - [25] O. Chepizhko and F. Peruani Phys. Rev. Lett. **111**, 160604, (2013).
  - [26] S. Mishra, S. Bhattacharya, B. Webb and E. G. D. Cohen, J. Stat. Phys. (2016).
  - [27] Antoine Bricard *et al.*, Nature Communications **6**, 7470 (2015).
  - [28] Fournier, R. L. 2007. Basic Transport Phenomena in Biomedical Engineering, New York, Taylor and Francis Group, LLC; Thiriet, M. 2007. Biology and Mechanics of Blood Flows Part II: Mechanics and Medical Aspects, Paris, Springer.